Journal of The Electrochemical Society, **153** (9) C616-C622 (2006)
0013-4651/2006/153(9)/C616/7/$20.00 © The Electrochemical Society

Electrodeposition of Cu in the PEI-PEG-Cl-SPS Additive System

Reduction of Overfill Bump Formation During Superfilling

S.-K. Kim, D. Josell, and T. P. Moffat*,z

National Institute of Standards and Technology, Materials Science and Engineering Laboratory, , Gaithersburg, Maryland 20899, USA

The impact of branched polyethyleneimine (PEI) on Cu electrodeposition from an acidified cupric sulfate electrolyte containing a combination of superfilling additives, specifically polyethylene glycol, bis(3-sulfopropyl)disulfide, and chloride (PEG–Cl–SPS), is examined. Electroanalytical measurements reveal that adsorption of cationic PEI leads to inhibition of the metal deposition reaction to an extent similar to that provided by PEG–Cl adsorption. However, unlike the PEG–Cl suppressor, PEI is shown to deactivate adsorbed SPS accelerator. As a result, addition of PEI quenches the hysteretic voltammetric response that is a signature of competitive adsorption in the PEG–Cl–SPS additive system. Trench-filling experiments in a PEI–PEG–Cl–SPS electrolyte demonstrate that the deactivating interaction between PEI adsorption and adsorbed SPS can be optimized to prevent overfill bump formation without substantial detrimental impact on bottom-up, void-free feature filling.
 [DOI: 10.1149/1.2216356]

Manuscript submitted February 16, 2006; revised manuscript received April 28, 2006. Available electronically July 5, 2006.

The use of organic additives to control the chemistry and mechanism of Cu electrodeposition permits present-day fabrication of interconnects for microelectronic devices and related packaging technologies. In particular, small concentrations of organic additives in the copper sulfate–sulfuric acid electrolyte used for deposition in trenches and vias permit defect-free, bottom-up filling. This applies to both Damascene and printed circuit board processing, including features ranging from 40 nm to 100 μm in size. Electrolytes containing constituents that compete to suppress and accelerate the Cu deposition rate [e.g., polyethylene glycol–chloride (PEG–Cl) and bis(3-sulfopropyl)disulfide–Cl (SPS–Cl), respectively] have been widely used and are receiving much attention from the research community. A quantitative description known as the curvature enhanced adsorbate coverage (CEAC) model is able to accurately predict this superfilling behavior by convolving the effects of competitive adsorption and area change on the metal deposition rate.[1]

Under appropriate processing conditions, robust bottom-up filling may be obtained using the PEG–Cl–SPS additive system. However, "overfill" bumps form above the superfilled features as a result of "momentum plating"; as explained by the CEAC model, this is due to the enhanced coverage of the adsorbed accelerator on the rapidly advancing bottom surface that also underlies the bottom-up feature-filling dynamic. The undesired topography can negatively impact subsequent planarization processes that are used in the fabrication of submicrometer interconnects for microelectronics. Significant research has therefore been devoted to amelioration of the overshoot phenomenon associated with bottom-up superfilling.[2-9] The central requirement for controlling bump formation is the removal or deactivation of the accelerator that has accumulated on the rapidly advancing bottom surface during feature filling. To preserve defect-free filling, it is evident that the deactivation process should only become dominant after the feature is filled. Strategies that have been proposed include addition of deposition-rate-inhibiting additives,[2-5] electrochemical treatments such as pulse plating,[2,6] chemical-mechanical action,[7] and multistep deposition processes that first optimize feature filling and then attenuate the superfilling dynamic by plating in the presence of a deactivating agent.[2,8,9]

Additives used to control overfill bump formation[2-4] have been referred to as "levelers." This is the case despite the feature sizes being incongruent with the application of conventional diffusion–adsorption–consumption leveling constructs and experimentally observed feature filling being inconsistent with their predictions.[10] In fact, it was recently suggested that these leveling additives actually control overfill bump formation through a variant of the CEAC area change mechanism that underlies the superfilling process itself.[5] In the CEAC-based model, deposition rate-inhibiting leveler (LEV) in the LEV–PEG–Cl–SPS system was assumed to deactivate SPS either by adsorption from solution or by related lateral interactions that accompany area reduction of advancing concave surfaces, analogous to the interplay between SPS and adsorbed PEG–Cl inhibitor already utilized in successful applications of CEAC-based models to the leveler-free, PEG–Cl–SPS system. Significantly, the proposed CEAC-based model predicted not only bump reduction in the presence of leveling additives but also enhanced inhibition in regions with high densities of features, also previously observed but unexplained. Steric hindrances to the transport of large leveler and suppressor macromolecules into the features, which might become important as feature sizes shrink toward the 10 nm range,[3,11] was not considered.

Numerous levelers have been identified and categorized.[2-9,12-15] However, much remains to be learned concerning the interactions between levelers and the other additives used for feature superfilling. To this end, the present study investigates the use of branched polyethyleneimine (PEI) as a leveler for controlling bump formation over features filled in electrolytes containing superfilling accelerator and supressor additives. PEI used in this study is a highly branched nitrogen-bearing weak polyelectrolyte with a $pK_a(pH) \approx 10.4$.[16] Acquisition of positive charge through protonation of the imine groups is anticipated upon addition to the acidic Cu deposition bath.[16] The N lone pair may also interact with Cu^{2+}, Cu^{+}, as well as the Cu surface, although protonation is expected to overwhelm metal ion complexation in the acidic plating electrolyte.[17] Voltammetry and chronoamperometry were used to study the impact of cationic PEI on Cu deposition kinetics in the absence and presence of various combinations of the superfilling additives. Filling of submicrometer-wide trenches during electrodeposition in a complete PEI-PEG-Cl-SPS system was used to directly assess the impact of PEI on overfill bump formation.

Experimental

The base electrolyte used for all electrochemical measurements was 0.16 mol/L $CuSO_4 \cdot 5H_2O$ and 1.8 mol/L H_2SO_4 in 18 MΩ cm deionized water. The organic additives studied were: 88 μmol/L PEG (3400 Mw; Aldrich[1]), 1 mmol/L NaCl (Fisher), 50 μmol/L $Na_2[SO_3(CH_2)_3S]_2$ (SPS; Raschig, Inc.), and 0–100 μmol/L PEI (

* Electrochemical Society Active Member.
z E-mail: thomas.moffat@nist.gov

[1]The names of companies and products are included for completeness of description. They do not imply NIST endorsement.

1800 Mw, branched; Alfa Aesar). All additives were added to the plating electrolyte by dilution from stock solutions of the additive dissolved in the $CuSO_4$-H_2SO_4 base electrolyte.

Slow-sweep cyclic voltammetry (1 mV/s) was used to characterize the impact of PEI on the Cu deposition kinetics. Electrolytes containing various combinations of additives were examined, namely, (*i*) additive-free, (*ii*) Cl-PEI, (*iii*) PEG-Cl-PEI, and (*iv*) PEG-Cl-SPS-PEI electrolytes. The working electrode for the electrochemical measurements was an oxygen-free high-conductivity Cu plate polished to 1200 grade SiC paper in deionized water. The plate was masked with 3M plater's tape, leaving an exposed circular area of 2.62 cm^2. A similar Cu plate was used as the counter electrode. To prevent perturbation of the working electrode by anode by-products, the working and counter electrode compartments were separated from each other using a Nafion 417 membrane.[18]

Deposition on Cu electrodes that had been pretreated in various PEI solutions was used to explore the impact of adsorbed PEI on the Cu deposition reaction. Different derivatization treatments were examined to probe the influence of potential on PEI adsorption. A Pt counter electrode and saturated calomel reference electrode were used during the controlled-potential derivatization treatments. The impact of the preadsorbed PEI on Cu deposition was assessed through voltammetric analysis of Cu deposition on the derivatized substrates in additive-free electrolyte. Consumption of the preadsorbed PEI was studied during Cu deposition in the presence of superfilling additives.

PEI deactivation of adsorbed SPS was also explored through comparison of voltammetry from Cu deposition on SPS derivatized electrodes in PEG–Cl containing electrolytes with and without 0.1 μmol/L PEI. The SPS derivatization was accomplished by suspending the Cu electrodes for 60 s under open-circuit conditions in a solution containing 500 μmol/L SPS + 1.8 mol/L H_2SO_4.

Copper deposition on wafers patterned with submicrometer trenches was examined to probe the efficacy of PEI for controlling overfill bump formation; cross-sectioned specimens were examined using a Hitachi S-4700-II field emission scanning electron microscope (FESEM). The substrates included a 50 nm thick sputtered Cu seed over a 12 nm thick Ta diffusion barrier on the patterned SiO_2 dielectric. Because of step-coverage limitations, the thickness of the sputtered seed was reduced to ~3 nm on the sidewalls. The trenches were between 230 and 250 nm deep and ranged from 120 to 70 nm in width at the bottom. Because the trench sidewalls were sloped, the width at midheight is used to estimate aspect ratios that vary between 2.0 and 3.0. All Cu electrodeposition was performed at −0.250 V vs saturated calomel electrode (SCE), the specimens immersed in the electrolyte at potential to minimize corrosion of the Cu seed layer. Feature filling was studied as a function of PEI concentration. For concentrations where bump formation was attenuated without significantly impacting bottom-up superfilling, deposition was also studied as a function of time.

Results and Discussion

PEI addition.— The influence of PEI on the voltammetric behavior during Cu electrodeposition from an otherwise additive-free electrolyte is shown in Fig. 1a. The PEI additions inhibit the Cu deposition reaction, with substantial suppression evident even at PEI concentration as low as 0.05 μmol/L. Significantly, for PEI concentrations less than 1 μmol/L, the initial current density of the forward scan (i.e., just below +40 mV) is little different from that observed in the absence of PEI; this suggests that negligible PEI is transferred to the surface during immersion through the air–electrolyte interface. Consistently, addition of PEI to the electrolyte induced no change of foaming during gas sparging, suggesting negligible surface segregation occurs at the air–water interface (unlike the case upon PEG addition). The onset of significant inhibition is apparent as the potential is scanned below −0.05 V SCE, the inhibition increasing monotonically with PEI concentration. For the more dilute PEI concentrations, increased suppression on the return sweep, consistent with additional PEI accumulation, results in hysteretic behavior; for concentrations above 5 μmol/L PEI the inhibition effect approaches saturation. The absence of significant changes at higher PEI concentration indicates that formation of the blocking layer occurs rapidly upon immersion in these solutions. The strong suppression of metal deposition provided by PEI is ascribed to interaction between charged imine groups and the copper surface.[16,19]

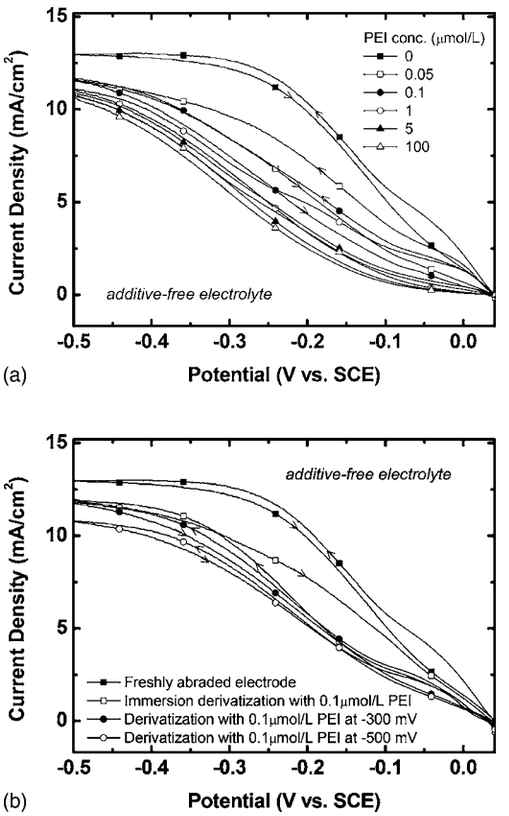

Figure 1. (a) Slow-sweep voltammetry of Cu deposition from 0.16 mol/L $CuSO_4$ + 1.8 mol/L H_2SO_4 electrolyte containing various concentrations of PEI. The curves were obtained with a scan rate of 1 mV/s. (b) Voltammetric curves for Cu deposition on PEI-derivatized electrodes. The electrodes were derivatized as follows: (open squares) immersion into 0.1 μmol/L PEI + 1.8 mol/L H_2SO_4 solution for 1 min (open-circuit condition) and immersion into the same solution for 1 min at potential −300 mV (black circle) and −500 mV (open circle) vs SCE, respectively. The voltammetric curves were obtained in the additive-free $CuSO_4$–H_2SO_4 electrolyte at 1 mV/s.

In order to gain more insight into the dynamics of PEI adsorption and the subsequent consumption of the adsorbate, a series of PEI derivatization experiments were performed. The electrode surfaces were derivatized by immersion in 1.8 mol/L H_2SO_4 and 0.1 μmol/L PEI for 60 s under open-circuit conditions or at an applied potential of −0.300 or −0.500 V SCE; a H_2SO_4 solution was used in the derivatization procedure to minimize changes in the charged monomer fraction and conformation of the adsorbed PEI during subsequent immersion into the Cu deposition electrolyte. The effect of the various PEI pretreatments on the rate of Cu electrodeposition in the additive-free electrolyte is summarized in Fig. 1b. The derivatized electrodes exhibit a similar degree of inhibition on the first negative-going voltammetric sweep. Again the extent of inhibition is quite remarkable given the small concentration of PEI and derivatization time in the derivatization electrolyte. In comparison of Fig. 1b to 1a, the three different derivatization potentials yield inhibition of Cu deposition on the negative-going sweep that is very similar to that observed during copper electrodeposition in the presence of 0.1 μmol/L PEI. Indeed, inhibition on the derivatized specimens

even after 190 s of copper deposition (i.e., at −0.15 V on the negative-going sweep) is similar to that obtained by deposition in the 0.1 μmol/L-PEI-containing electrolyte for the same period. Integrating the current from +40 to −150 mV, the inhibition provided by the derivatized PEI layer is sustained during Cu deposition equivalent to ~0.42 C/cm^2 or ~155 nm over 190 s. In fact, the longevity of the PEI derivatized adlayer extends to significantly greater thicknesses, as is apparent from the sustained inhibition of the derivatized electrodes during the reverse sweep. Comparison of the forward and reverse sweeps of the derivatized electrodes reveals that the stability of the blocking PEI layer is enhanced by pretreatment at more negative potentials; specimens derivatized at −0.3 and −0.5 V exhibit return scans that are nearly identical with the negative-going scans while deposition on the specimen derivatized at open circuit is less inhibited on the return sweep, yielding the hysteretic η-*i* response in Fig. 1b. The loss of inhibition may arise from either incorporation of the adlayer into the growing Cu deposit or desorption into the electrolyte. While polymer adsorption on metal surfaces is often thought to be highly irreversible due to the low probability of progressively, or simultaneously, desorbing the macromolecule at multiple attachment points[20,21] if the attachment chemistry is redox active, a significant potential dependence is to be expected.

The observed impact of derivatization potential may reflect small changes in coverage or, more likely, differences in the conformation and nature of the surface attachment of the adsorbed polymer. One significant difference between derivatization at open circuit and more negative potentials is the relative concentrations of Cu^+ and Cu^{2+} near the electrode surface that might act to hinder or enhance PEI adsorption on the surface and influence its conformation. While neutral PEI has a lone pair of electrons available for complexation with copper ions, the polyelectrolyte is heavily protonated at low pH and complexation with Cu^{++} or Cu^+ is likely to be minimal.[17] Another factor to be considered is sulfate adsorption and how its potential dependent character interacts with PEI adsorption.

PEI-Cl addition.— Chloride addition to a $CuSO_4$ plating bath is known to catalyze the copper deposition reaction through the formation of a Cu–Cl–Cu^{2+} bridge complex that mediates Cu^{2+} reduction.[22,23] Chloride is also an important coadsorbate required for the formation of the blocking PEG–Cl and catalytic SPS–Cl surface species that are central to the Cu superfilling process. In contrast, it is clear from the data in Fig. 1 that PEI does not require halide to produce strong inhibition of copper deposition, and addition of dilute chloride would not be expected to perturb the conformation or charge of PEI, both of which are set by the ionic strength and pH of the electrolyte.[16]

The influence of 1 mmol/L chloride on formation of the blocking PEI layer is examined in Fig. 2. While comparison with Fig. 1a reveals the acceleration provided by chloride addition to the PEI-free electrolyte, inhibition of the Cu deposition is still evident on the negative-going sweep for all nonzero PEI concentrations. However, unlike the halide-free case, significant acceleration of the deposition reaction is apparent on the return sweep for PEI concentrations below 1 μmol/L. The associated hysteresis indicates a competition exists between adsorbed/adsorbing accelerating Cl^-[22,23] and suppressing PEI; the crossing point at −0.280 V for 1 μmol/L PEI suggests a potential or deposition-rate dependence for consumption or desorption of at least one of the adsorbates. The disruption of PEI inhibition by chloride is overwhelmed when the PEI concentration exceeds 5 μmol/L. This value is similar to the saturation threshold observed in the chloride-free case and yields Cu deposition kinetics that are indistinguishable. This indicates that chloride does not play a significant role in PEI-induced inhibition at saturation.

PEI–PEG–Cl addition.— The strong suppression of the copper deposition reaction induced by PEG and Cl^- additions is clear in comparison of the PEI-free results of Fig. 3 and 1. Addition of PEI leads to a minor perturbation of the voltammetric response, with

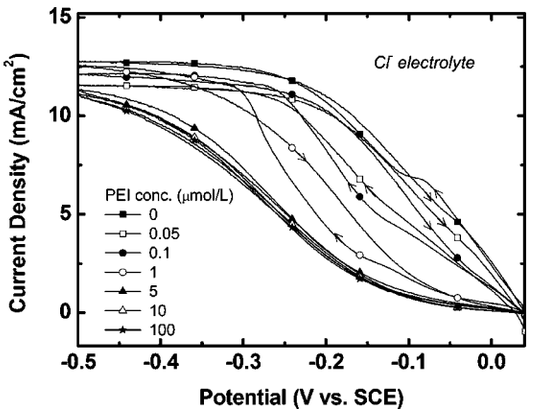

Figure 2. Effects of PEI on the voltammetric response during Cu deposition in the presence of Cl^-. The electrolyte was composed of 0.16 mol/L $CuSO_4$ + 1.8 mol/L H_2SO_4 + 1 mmol/L NaCl and the scan rate was 1 mV/s.

only a slight increase in inhibition visible in Fig. 3 for the highest PEI concentrations. It is difficult to ascertain the relative contribution of the two species to inhibition because the saturated response for the PEG–Cl and PEI system are very similar; this supports the use of identical deposition kinetics on leveler-saturated and PEG-Cl suppressor-saturated surfaces in the recent CEAC-based modeling of the impact of leveling additives on overfill bump formation.[5] Nonetheless, the reduced suppression visible at the lower PEI concentrations in Fig. 1 makes it clear that the deposition kinetics on the planar electrodes are under the control of PEG-Cl, at least for PEI concentrations between 0 and 1 μmol/L that will be seen to be most relevant to superfilling applications.

PEI–PEG–Cl–SPS.— The main characteristic of the three-component PEG–Cl–SPS electrolyte is competition between the inhibiting PEG–Cl and accelerating SPS–Cl species for electrode surface sites. For typical additive concentrations used in superfilling applications, specimen immersion leads to rapid formation of a blocking PEG–Cl layer that is subsequently disrupted and displaced by potential-dependent adsorption of SPS.[1] The acceleration of the deposition rate that results from gradual disruption of the blocking layer by the accumulating SPS continually shifts the metal deposition toward more positive potentials and yields the hysteretic voltammetric response visible in Fig. 4 for electrolyte free of PEI. In contrast, the addition of 0.05 μmol/L PEI displaces the metal depo-

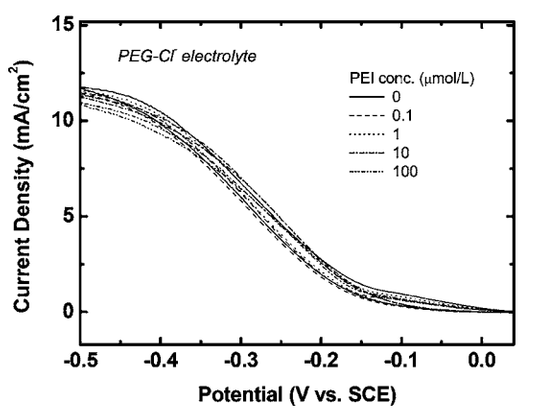

Figure 3. Effects of added PEI on the voltammetric response during Cu deposition in the presence of PEG and Cl^-. The electrolyte was composed of 0.16 mol/L $CuSO_4$ + 1.8 mol/L H_2SO_4 + 88 μmol/L PEG + 1 mmol/L NaCl and the scan rate was 1 mV/s.

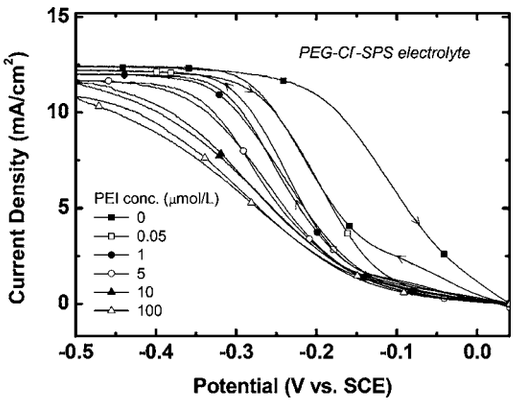

Figure 4. Voltammetric curves detailing the effect of PEI on Cu deposition from a PEG-Cl-SPS electrolyte. Quenching of the hysteretic behavior of the PEG–Cl–SPS electrolyte is evident, along with the displacement of the curves toward higher overpotentials. The electrolyte was composed of 0.16 mol/L $CuSO_4$ + 1.8 mol/L H_2SO_4 + 88 μmol/L PEG + 1 mmol/L NaCl + 50 μmol/L SPS and the scan rate was 1 mV/s.

sition back toward more negative potentials and substantially decreases the area enclosed by the hysteretic loop. Evidently, PEI hinders SPS activation of the electrode. As the PEI concentration is increased, the extent of inhibition progressively increases and the hysteretic response is effectively quenched for PEI concentrations above 1 μmol/L. As the PEI concentration increases further, displacement of the curves toward negative potential occurs. The resilience of acceleration at the more negative potentials is due to more competitive SPS adsorption resulting from adsorption kinetics that increase with overpotential, as assessed in prior work.[1] As the PEI concentration exceeds 10 μmol/L, the system approaches the characteristics of a PEI-saturated surface for the conditions studied.

The behavior of the PEI–PEG–Cl–SPS system was also examined by multicycle voltammetry. As shown in Fig. 5, a near-steady-state result is attained for all PEI concentrations after one cycle, and the hysteresis is essentially extinguished for PEI concentrations in excess of 1 μmol/L.

The possibility of ion-pairing interactions between cationic polymers and anionic surfactants such as SPS has received significant attention in the literature.[24,25] For reference, PEI used in this study has approximately 40 imine sites per molecule, of which a significant fraction should be available for ion pairing with appropriate anionic species. In terms of total cationic–anionic site count, a PEI concentration of 2.5 μmol/L matches the numbers of anionic sites associated with 50 μmol/L SPS. While significant ion pairing between PEI and SPS is not expected in the strongly supported 1.8 mol/L H_2SO_4 electrolyte, such interactions might be expected to play an important role at surfaces.[24,25]

Additional derivatization experiments were performed in order to investigate the nature of SPS–PEI interaction in more detail. Results for electrodes derivatized by immersion in 500 μmol/L SPS for 1 min and then transferred for copper deposition in the presence of PEG–Cl with and without 0.1 μmol/L PEI are shown in Fig. 6a. Copper deposition on the freshly immersed SPS derivatized electrode in PEG–Cl is very active but undergoes marked deactivation at −0.045 V SCE that is related to SPS consumption, as previously detailed elsewhere.[1] At more negative potentials the deactivation process continues, albeit with a much smaller rate constant. In contrast, when the experiment is repeated in the presence of 0.1 μmol/L PEI, the reactivity of the electrode is rapidly quenched such that by −0.150 V the electrode response approaches the suppressed response exhibited by the freshly prepared bare Cu electrode with its $PEG–Cl^-$/PEI blocking layer. This unambiguously demonstrates that PEI adsorption deactivates adsorbed SPS. Because the catalytic activity of SPS is associated with the anionic sulfonate end group,[1]

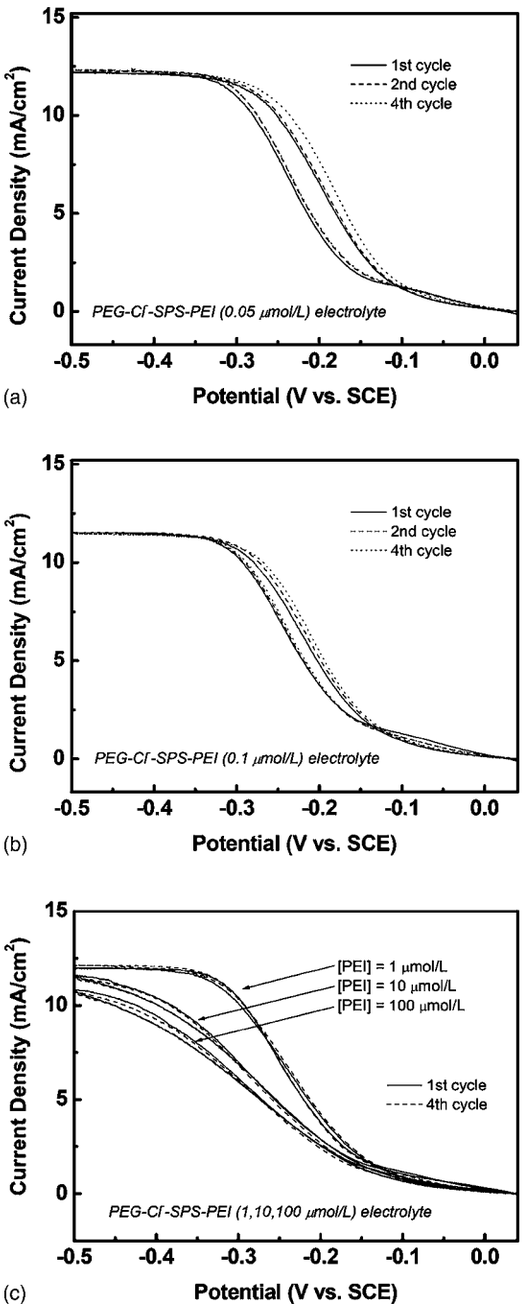

Figure 5. Multicycle voltammetry for copper deposition in the PEI-PEG-Cl-SPS system as a function of PEI concentration. The base electrolyte was 0.16 mol/L $CuSO_4$ + 1.8 mol/L H_2SO_4 + 88 μmol/L PEG + 1 mmol/L NaCl + 50 μmol/L SPS to which was added (a) 0.05, (b) 0.1, (c)1, 10, and 100 μmol/L PEI, respectively.

quenching of its activity by ion pairing with the cationic N^+ sites of PEI is the most likely mechanism. The increased steric hindrance through coupling with highly branched PEI may also affect the related reactions[26-28] between SPS and Cu(I)/Cu(II). As the deactivated electrode reverts to the characteristics of the PEG–Cl system it is possible that the SPS-PEI complex is buried in the growing deposit. This would be congruent with a literature report[29] detailing a monotonic increase in S and N content in the deposit with the concentration of N-bearing leveler concentration used in the electrolyte.

Further insight into the PEI consumption process may also be

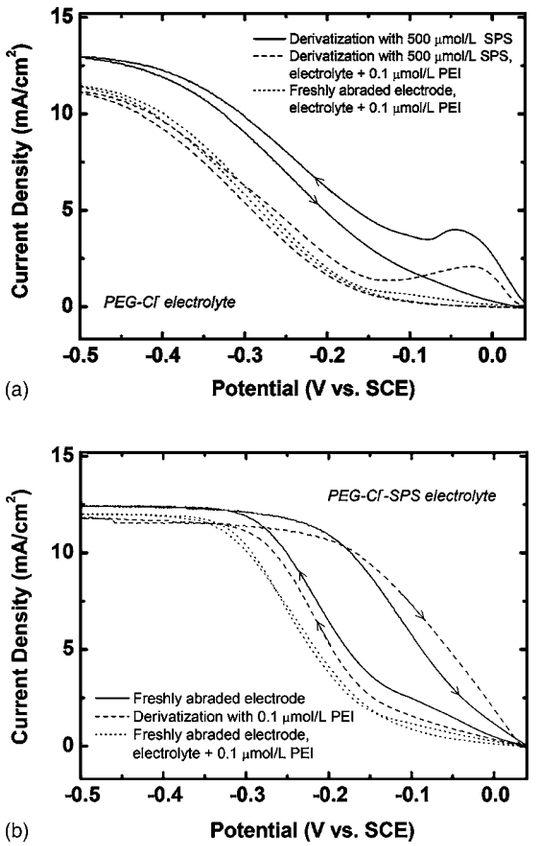

Figure 6. (a) Deactivation of an SPS-derivatized electrode during voltammetric Cu deposition in a PEI-containing electrolyte. Derivatization of the Cu electrode was performed in 500 μmol/L SPS + 1.8 mol/L H_2SO_4 solution for 1 min. The electrolyte was composed of 0.16 mol/L $CuSO_4$ + 1.8 mol/L H_2SO_4 + 88 μmol/L PEG + 1 mmol/L NaCl. The response of the SPS-derivatized electrodes in the absence and presence of 0.1 μmol/L PEI is compared. (b) Deactivation of a PEI-derivatized electrode in the presence of superfilling additives. The derivatization of the Cu electrode was performed in 0.1 μmol/L PEI + 1.8 mol/L H_2SO_4 solution for 1 min under open-circuit conditions. The electrolyte was composed of 0.16 mol/L $CuSO_4$ + 1.8 mol/L H_2SO_4 + 88 μmol/L PEG + 1 mmol/L NaCl + 50 μmol/L SPS. For comparison, Cu deposition on a fresh electrode in the 0.1 μmol/L PEI + 0.16 mol/L $CuSO_4$ + 1.8 mol/L H_2SO_4 + 88 μmol/L PEG + 1 mmol/L NaCl + 50 μmol/L SPS electrolyte is also presented.

garnered by examining the behavior of a PEI-derivatized electrode during copper deposition in the PEG–Cl–SPS system. Voltammetry from a freshly polished electrode that was pretreated for 60 s in 0.1 μmol/L PEI + 1.8 mol/L H_2SO_4 solution and then transferred to the PEG–Cl–SPS plating electrolyte is shown in Fig. 6b. Consistent with Fig. 4, initial deposition at low overpotentials is significantly inhibited, whereas, as the potential becomes more negative and the SPS adsorption kinetics increase, the deposition rate accelerates to yield a hysteretic voltammetric response characteristic of the PEG–Cl–SPS system. This demonstrates that SPS can adsorb and deactivate the preadsorbed PEI layer, thereby accelerating the deposition reaction. In contrast, if PEI is present in the electrolyte, a completely different response is observed whereby the continuous flux of PEI prevents electrode activation by either interfering with SPS adsorption or, more likely, quenching the activity of the end group of adsorbed SPS. Thus, the derivatization experiments demonstrate that PEI adsorption is associated with deactivation of adsorbed SPS, and likewise, SPS adsorption contributes to deactivation of adsorbed PEI.

The PEI–PEG–Cl–SPS system was also examined by chrono-

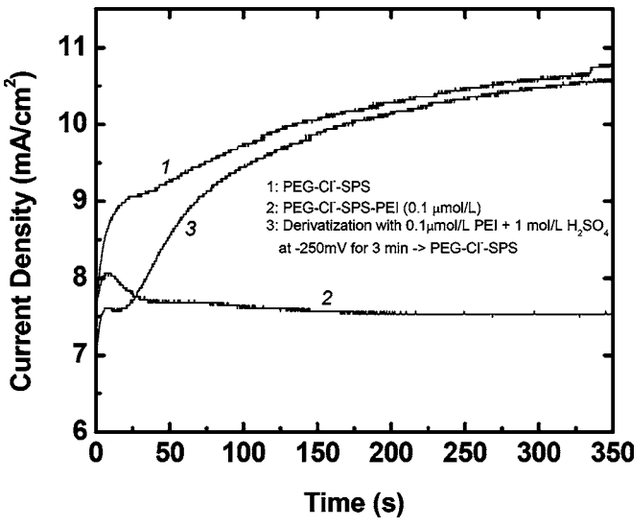

Figure 7. Chronoamperometry revealing the effect of PEI adsorption on copper deposition in the PEI-PEG-Cl-SPS system. In the absence of PEI a rising transient associated with PEG displacement by SPS adsorption is observed. PEI additions lead to quenching of the SPS activity. The depassivation of a PEI-derivitized electrode also shown indicates that SPS adsorption contributes to deactivation of PEI.

amperometry. As shown in Fig. 7, potentiostatic deposition at −0.250 V SCE in the PEG–Cl–SPS system yields a rising current transient associated with progressive displacement of the suppressing PEG–Cl layer by SPS adsorption. Deposition in the added presence of 0.1 μmol/L PEI results in sharp attenuation of this behavior, the rising transient passing through a maximum after 5 s and then decaying to a steady-state current that is only 70% of that observed in the absence of PEI. The chronoamperometric response of a PEI electrode that was derivatized by immersion at −0.250 V vs SCE in 0.1 μmol/L PEI for 180 s and then transferred for copper deposition in the PEG–Cl–SPS electrolyte is readily understood in terms of the PEI and PEI-free results. As seen in Fig. 7, deposition first proceeds at a rate consistent with that of a PEI suppressed surface, as determined from the steady-state value observed during extended plating in the PEI–PEG–Cl–SPS case. Then, after 23 s the current begins to increase in a manner consistent with that observed for a freshly polished electrode in the PEG–Cl–SPS system. As in the case of Fig. 6b, this demonstrates that the preadsorbed PEI is consumed during the passage of 0.17 C/cm^2 or the 63 nm equivalents of Cu deposition associated with the plateau. Such experiments provide an avenue for quantifying the SPS-dependent PEI consumption dynamics.

Understanding of the PEI–PEG–Cl–SPS system can be summarized as follows. The accelerating action of adsorbed SPS on Cu deposition has been previously ascribed to its ability to displace the passivating PEG layer that forms readily upon immersion into the PEG–Cl–SPS electrolyte. The anionic functionality of the sulfonate end group of SPS is a key element preventing the formation of the inhibiting PEG layer as well as sustaining SPS segregation at the growing interface.[1] The results of this study indicate that addition of the cationic polyelectrolyte PEI quenches the SPS activity, this effect being attributed to an ion-pairing interaction. Comparison to literature data[29] suggests that such an ion-pairing process may be an important step in the incorporation of both SPS and PEI (and/or their respective constituents) into the growing deposit; derivatization experiments presented above and elsewhere indicate that relatively minor incorporation of either species occurs in the absence of the other under conventional plating conditions (~10 mA/cm^2). These conclusions are also consistent with published measurements of sulfur and nitrogen incorporation in films grown in commercial suppressor–accelerator–leveler electrolyte systems.[29] Finally, in the

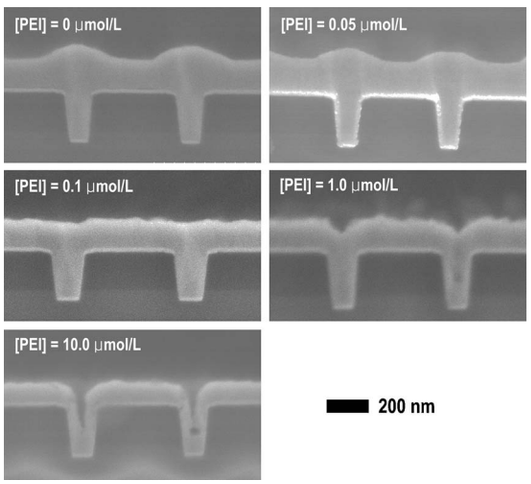

Figure 8. Cross-sectional FESEM images of the Cu deposition on the 120 nm wide trench patterns as a function of PEI concentration. Deposition was carried out at −0.250 V for 30 s in the electrolyte composed of 0.16 mol/L $CuSO_4$ + 1.8 mol/L H_2SO_4 + 88 μmol/L PEG + 1 mmol/L NaCl + 50 μmol/L SPS + 0–10 μmol/L PEI. Superfilling followed by attenuation of overfill bump formation is evident for $[PEI] \leq 0.1$ μmol/L, while a change in the deposition profile toward conformal growth occurs for $[PEI] \geq 1$ μmol/L.

absence of SPS, PEI yields suppression of Cu deposition, with deposition kinetics similar to those observed for PEG–Cl.

Trench Filling Experiments.— The characteristics outlined above for the PEI–PEG–Cl–SPS system are consistent with the requirements for controlling the momentum plating that leads to bump formation above trenches and vias during the Damascene metallization process. The impact of PEI additions on feature filling during deposition from the model PEI–PEG–Cl–SPS superfilling electrolyte was therefore examined.

Trench filling as a function of PEI concentration is shown in Fig. 8. In all cases, Cu was electrodeposited for 30 s at −0.250 V vs SCE in the PEI–PEG–Cl–SPS electrolyte. In the absence of PEI, overfill bumps are evident due to the enrichment of adsorbed SPS that accompanies area reduction during bottom-up trench filling. A more detailed explanation of the superconformal growth process may be found elsewhere.[1] The addition of 0.05 μmol/L PEI leads to a slight decrease in the size of the overfill bumps as PEI accumulation combined with area reduction during feature filling results in a slight attenuation of the SPS activity above the filled trenches. For 0.1 μmol/L PEI, twice as much PEI is expected to adsorb during feature filling. This additional increment leads to a complete attenuation of bump formation with no apparent degradation of the trench filling. For higher PEI concentrations, more extensive SPS deactivation occurs and the growth profile reverts to a conformal mode that yields undesirable seam and void formation within the trench. Thus, for the given trench geometry, potential, and electrolyte, 0.1 μmol/L PEI is close to the optimum value for minimizing bump formation without negatively impacting bottom-up feature filling.

To confirm that the 0.1 μmol/L PEI addition does not interfere with bottom-up feature filling, trench filling was examined as a function of deposition time. The bottom-up trench filling that is characteristic of superfilling is clear in Fig. 9. Thus, for this PEI concentration, bottom-up filling is not significantly perturbed. Furthermore, it is evident that the planar growth front is maintained during growth through 60 s.

The influence of varying feature size and separation was also examined over a limited range of midheight widths from 70 to 120 nm and feature separations 400–350 nm. The left side of Fig. 10 shows bump formation over three different arrays of filled

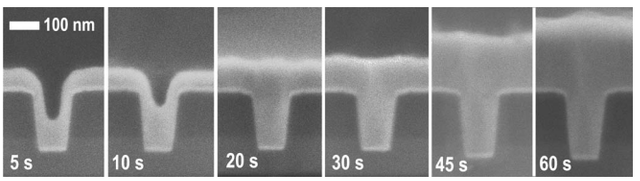

Figure 9. Cross-sectional FESEM images of the Cu deposition as a function of the deposition time in a 0.1 μmol/L PEI-PEG-Cl-SPS electrolyte. Deposition was carried out at −250 mV vs SCE for 5, 10, 20, 30, 45, and 60 s in the electrolyte composed of 0.16 mol/L $CuSO_4$ + 1.8 mol/L H_2SO_4 + 88 μmol/L PEG + 1 mmol/L NaCl + 50 μmol/L SPS + 0.1 μmol/L PEI. Prevention of bump formation without impact on superfilling is evident.

trenches in the absence of PEI; all are from the same specimen. The images reveal (c) the transitions from noninteracting bumps to (b) the first signs of overlap to (a) the acceleration between adjacent features due to CEAC-induced buildup of SPS on the concave surface formed between overfill bumps. Note particularly the thickness in the field between the features; the entire deposit in (a) is now thicker than the thickness in the field in (b) and (c).

In contrast, the addition of 0.1 μmol/L PEI effectively attenuates bump formation for the trench widths, spacings, and plating conditions examined; note particularly the uniform thickness of the field in Fig. 10d-f as compared to Fig. 10a-c. Close examination suggests slight bump formation over some of the trenches in Fig. 10d. This is consistent with the expectation of reduced PEI accumulation, and resulting increase of possible SPS enrichment by area change (CEAC), for the faster filling of these smallest features.[1]

The above experiments reveal several different aspects of the impact of feature size and spacing on bump control. The results also demonstrate that a leveler addition can greatly diminish the dispersion in the uniformity of thickness of the overburden film, an effect that simplifies the task of subsequent planarization processes.

Conclusions

The effect of polyethyleneimine on Cu deposition kinetics as well as its interaction with other superfilling additives and their combined effect on feature filling was studied. Electroanalytical measurements reveal that adsorption of cationic PEI leads to inhibition of the metal deposition reaction to an extent similar to that provided by PEG–Cl adsorption. However, unlike the PEG–Cl suppressor, PEI has the ability to deactivate the adsorbed SPS accelerator, presumably through an ion-pairing interaction between the cationic imine groups of the polyelectrolyte and the anionic tail group of the adsorbed SPS accelerator. In cyclic voltammetry, the PEI deactivation of adsorbed SPS manifests as a quenching of the hys-

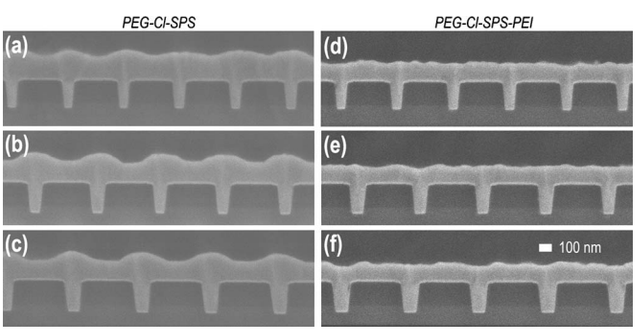

Figure 10. Cross-sectional FESEM images of Cu deposition as a function of the trench width and separation. The trenches have midheight widths ranging from 70 to 120 nm with depth between 230 and 250 nm. Deposition was carried out at −0.250 V for 30 s in the electrolyte composed of 0.16 mol/L $CuSO_4$ + 1.8 mol/L H_2SO_4 + 88 μmol/L PEG + 1 mmol/L NaCl + 50 μmol/L SPS + 0.1 μmol/L PEI.

teretic voltammetric response associated with competitive adsorption in a superfilling PEG–Cl–SPS-containing electrolyte. In trench-filling experiments, a remarkably low concentration of PEI (0.1 μmol/L) in the same superfilling electrolyte was shown to be effective for controlling bump formation that otherwise occurs above submicrometer features during superfilling. Although a quantitative comparison awaits an appropriate quantitative description for the dynamics of PEI adsorption and consumption, the electrochemical and trench-filling experiments are in qualitative agreement with a recently proposed CEAC model for four-component leveler-PEG–Cl–SPS systems.

Acknowledgments

The authors thank S. Claggett for assistance in preparation of specimens for FESEM.

National Institute of Standards and Technology assisted in meeting the publication costs of this article.

References

1. T. P. Moffat, D. Wheeler, M. Edelstein, and D. Josell, *IBM J. Res. Dev.*, **49**, 19 (2005).
2. B. Zheng, R. He, B. Mikkola, J. Wang, C. Long, C. Yu, Z.-W. Sun, E. Step, J. Chen, R. Emamai, Z. A. Wang, R. Nayak, T. Taylor, and G. Dixit, in *Proceedings of Advanced Metallization Conference 2001*, A. J. McKerrow, Y. Shacham-Diamand, S. Zaima, and T. Ohba, Editors, p. 197, MRS, Warrendale, PA (2001).
3. J. Reid, E. Webb, J. Sukamto, Y. Takada, and T. Archer, in *Electrochemical Processing in ULSI and MEMS*, H. Deligianni, S. T. Mayer, T. P. Moffat, and G. R. Stafford, Editors, PV 2004-17, p. 184, The Electrochemical Society Proceedings Series, Pennington, NJ (2005).
4. M. Hasegawa, Y. Negishi, T. Nakanishi, and T. Osaka, *J. Electrochem. Soc.*, **152**, C221 (2005).
5. T. P. Moffat, D. Wheeler, S.-K. Kim, and D. Josell, *J. Electrochem. Soc.*, **153**, C127 (2006).
6. S. K. Cho and J. J. Kim, Abstract 580, Electrochemical Society Meeting Abstracts, Los Angeles, CA, Oct 16–21, 2005.
7. M. Basol, *J. Electrochem. Soc.*, **151**, C765 (2004).
8. M. X. Yang, D. X. Mao, C. M. Yu, J. Dukovic, and M. Xi, *Solid State Technol.*, **46**, 37 (2003).
9. S.-K. Kim, S. Hwang, S. K. Cho, and J. J. Kim, *Electrochem. Solid-State Lett.*, **9**, C25 (2006).
10. P. C. Andricacos, C. Uzoh, J. O. Dukovic, J. Horkans, and H. Deligianni, *IBM J. Res. Dev.*, **42**, 567 (1998).
11. M. M. Gomez, J. M. Vara, J. C. Hernandez, R. C. Salvarrezza, and A. Arvia, *Electrochim. Acta*, **47**, 405 (2001).
12. E. D. Eliadis and R. C. Alkire, *J. Electrochem. Soc.*, **145**, 1218 (1998).
13. M. Wunsche, W. Dahms, H. Meyer, and R. Schumacher, *Electrochim. Acta*, **39**, 1133 (1994).
14. Y. Cao, P. Taephaisitphongse, R. Chalupa, and A. West, *J. Electrochem. Soc.*, **148**, C466 (2001); P. Taephaisitphongse, Y. Cao, and A. C. West, *J. Electrochem. Soc.*, **148**, C492 (2001).
15. W.-P. Dow, H.-S. Huang, M.-Y. Yen, and H.-C. Huang, *J. Electrochem. Soc.*, **152**, C425 (2005).
16. R. Meszaros, L. Thompson, M. Bos, and P. De Groot, *Langmuir*, **18**, 6164 (2002).
17. V. N. Kislenko and L. P. Oliynyk, *J. Polym. Sci., Part A: Polym. Chem.*, **40**, 914 (2002).
18. T. P. Moffat, B. Baker, D. Wheeler, and D. Josell, *Electrochem. Solid-State Lett.*, **6**, C59 (2003).
19. P. Somasundaran and S. Krishnakumar, *Colloids Surf., A*, **123–124**, 491 (1997).
20. M. A. Cohen Stuart, C. W. Hoogendam, and A. de Keizer, *J. Phys. Condens. Matter*, **9**, 7767 (1997).
21. R. R. Netz and D. Andelman, in *Encyclopedia of Electrochemistry*, E. Gileadi, M. Urbakh, A. J. Bard, and M. Stratmann, Editors, p. 282, VCH-Wiley, Inc., Weinheim (2002).
22. Z. Nagy, J. P. Blaudeau, N. C. Hung, L. A. Curtiss, and D. J. Zurawski, *J. Electrochem. Soc.*, **142**, L87 (1995).
23. M. Yokoi, S. Konishi, and T. Hayashi, *Denki Kagaku oyobi Kogyo Butsuri Kagaku*, **51**, 460 (1983).
24. J. Penfold, I. Tucker, R. K. Thomas, and J. Zhang, *Langmuir*, **21**, 10061 (2005).
25. J. Penfold, I. Tucker, and R. K. Thomas, *Langmuir*, **21**, 11757 (2005).
26. J. J. Kim, S.-K. Kim, and Y. S. Kim, *J. Electroanal. Chem.*, **542**, 61 (2003).
27. A. Frank and A. J. Bard, *J. Electrochem. Soc.*, **150**, C244 (2003).
28. S.-K. Kim and J. J. Kim, *Electrochem. Solid-State Lett.*, **7**, C98 (2004).
29. C. Witt, J. Srinivasan, and R. Carpio, in *Electrochemical Processing in ULSI and MEMS*, H. Deligianni, S. T. Mayer, T. P. Moffat, and G. R. Stafford, Editors, PV 2004-17, p. 57, The Electrochemical Society Proceedings Series, Pennington, NJ (2005).